Physics and Imaging in Radiation Oncology 30 (2024) 100583

Contents lists available at ScienceDirect

Physics and Imaging in Radiation Oncology

journal homepage: www.sciencedirect.com/journal/physics-and-imaging-in-radiation-oncology

Original Research Article

Comparing different boost concepts and beam configurations for proton therapy of pancreatic cancer

Taiki Takaoka [a,*], Takeshi Yanagi [b], Shinsei Takahashi [b], Yuta Shibamoto [b], Yuto Imai [a,b], Dai Okazaki [a], Masanari Niwa [a], Akira Torii [a], Nozomi Kita [a], Seiya Takano [a], Natsuo Tomita [a], Akio Hiwatashi [a]

[a] Department of Radiology, Nagoya City University Graduate School of Medical Sciences, Nagoya, Japan
[b] Department of Radiation Oncology, Narita Memorial Proton Center, Toyohashi, Japan

ARTICLE INFO

Keywords:
Pancreatic cancer
Proton therapy
Pencil-beam scanning
Field-in-field
Simultaneous integrated boost

ABSTRACT

Background and Purpose: Interfractional geometrical and anatomical variations impact the accuracy of proton therapy for pancreatic cancer. This study investigated field-in-field (FIF) and simultaneous integrated boost (SIB) concepts for scanned proton therapy treatment with different beam configurations.
Materials and Methods: Robustly optimized treatment plans for fifteen patients were generated using FIF and SIB techniques with two, three, and four beams. The prescribed dose in 20 fractions was 60 Gy(RBE) for the internal gross tumor volume (IGTV) and 46 Gy(RBE) for the internal clinical target volume. Verification computed tomography (vCT) scans was performed on treatment days 1, 7, and 16. Initial treatment plans were recalculated on the rigidly registered vCTs. $V_{100\%}$ and $D_{95\%}$ for targets and D^{3}_{2cm} for the stomach and duodenum were evaluated. Robustness evaluations (range uncertainty of 3.5 %) were performed to evaluate the stomach and duodenum dose-volume parameters.
Results: For all techniques, IGTV $V_{100\%}$ and $D_{95\%}$ decreased significantly when recalculating the dose on vCTs ($p < 0.001$). The median IGTV $V_{100\%}$ and $D_{95\%}$ over all vCTs ranged from 74.2 % to 90.2 % and 58.8 Gy(RBE) to 59.4 Gy(RBE), respectively. The FIF with two and three beams, and SIB with two beams maintained the highest IGTV $V_{100\%}$ and $D_{95\%}$. In robustness evaluations, the ΔD^{3}_{2cm} of stomach was highest in two beams plans, while the ΔD^{3}_{2cm} of duodenum was highest in four beams plans, for both concepts.
Conclusion: Target coverage decreased when recalculating on CTs at different time for both concepts. The FIF with three beams maintained the highest IGTV coverage while sparing normal organs the most.

1. Introduction

Various cancer treatment strategies, including intraoperative radiotherapy, have been attempted to improve the prognosis of unresectable pancreatic cancer [1,2]. The superiority of chemoradiotherapy remains controversial [3]; however, particle therapy combined with systemic chemotherapy improved overall survival compared to chemoradiotherapy using X-ray beams [4,5]. Several studies have demonstrated that dose escalated particle therapy positively affected clinical outcomes in patients with pancreatic cancer [5,6], and proton therapy is considered a promising treatment strategy for these patients [7]. Proton therapy using pencil-beam scanning (PBS) can deliver higher doses to targets compared to conventional radiotherapy [8], which is critical to improve the local control rate.

Particle therapy for abdominal targets is very complex because organ motion and bowel gas movement may seriously affect particle range, attenuation, and spot placement [9–13]. Various beam directions have been investigated for carbon-ion radiotherapy of pancreatic cancer [14,15], but studies on proton therapy are limited [16]. This study [16] compared PBS proton therapy using two or three beam techniques and reported that the three-beam technique achieved a homogeneous dose distribution in the target. However, there is no consensus on the optimal beam arrangement in proton therapy for pancreatic cancer even using three beams showed to achieve a homogenous dose distribution in the target [16]. To identify suitable beam arrangements robustness evaluation is essential as recently demonstrated [17,18]. The simultaneous

* Corresponding author at: Department of Radiology, Nagoya City University Graduate School of Medical Sciences, 1 Kawasumi, Mizuho-cho, Mizuho-ku, Nagoya 467-8601, Japan.
E-mail address: gkwtt762@yahoo.co.jp (T. Takaoka).

https://doi.org/10.1016/j.phro.2024.100583
Received 30 October 2023; Received in revised form 26 April 2024; Accepted 26 April 2024
Available online 27 April 2024

integrated boost (SIB) technique is more commonly used to deliver higher doses to targets. Another technique is the field-in-field (FIF) method, which consists of main field and sub-fields. The FIF technique is not commonly used for PBS proton therapy but showed promising results for breast cancer photon therapy compared to SIB [19,20]. We aimed to evaluate whether the FIF technique was equivalent to the SIB technique regarding dose distributions in PBS proton therapy.

2. Material and methods

2.1. Study design and patient characteristics

Within this study we employed the imaging and structure data sets of fifteen patients with pancreatic cancer who had been treated with proton therapy at our institution between July 2020 and August 2022. The median age of the patients was 75 years (58–84 years), while the complete patient characteristics are summarized in Table S1. The median volumes of the gross tumor volume (GTV) and clinical target volume (CTV) were 28 cm^3 (5–98 cm^3) and 112 cm^3 (49–267 cm^3), respectively. The median volumes of the internal GTV (IGTV) and internal CTV (ICTV) were 39 cm^3 (18–136 cm^3) and 153 cm^3 (69–364 cm^3), respectively. The prescribed median doses to the IGTV and ICTV were a biologically-weighted dose of 60 Gy(RBE) and 46 Gy(RBE), respectively, in 20 fractions. In the clinical treatment, some patients received treatment plans prioritizing the safety of organs like the stomach and duodenum, even if the target coverage might not meet constraints. For this in-silico study dedicated treatment pans were created fulfilling comparable clinical goals for the target regions and organs at risk (OARs) instead of employing the clinical treatment plans. A compact proton beam machine with single-field optimization PBS (Proteus® One, Ion Beam Applications S.A., Belgium) were used. Written informed consent was obtained from all patients for this treatment planning study. This study was approved by the institutional review board at Narita Memorial Hospital (No. R041041) and has been conducted in compliance with the guidelines of the Helsinki Declaration.

2.2. Immobilization, imaging, and treatment planning

Patients were immobilized in a supine position with a body vacuum bag system (ESFORM; Engineering System Co., Ltd. Nagano, Japan), and four-dimensional computed tomography (4DCT) (SOMATOM Definition AS; Siemens Healthineers AG, Bayern, Germany) scans were performed nine days prior to the first fraction for treatment planning. The 4DCT scan were acquired with a 2 mm slice thickness under shallow breathing. The CT setting for the abdominal scans were 97.5 mAs and 120 kV. All patients were trained to breathe shallowly and abdominal compression was used to minimize the respiratory movements. The stoichiometric calibration method was used to create the Hounsfield unit-stopping power ratio calibration curve. Contouring was conducted on contrast-enhanced CT images and/or ^{18}F-fluorodeoxyglucose positron emission tomography images. The GTV was defined as visible tumor, and the CTV was defined as the GTV plus the prophylactic lymph node area around the pancreas. The GTV and CTV were delineated in all phases of the 4DCT which consisted of 10 phases, and the delineations were summed up. The delineations were defined as IGTV and ICTV. Delineated OARs at the end-expiratory phase CT were the stomach, duodenum, small bowel, large bowel, bilateral kidneys, spinal cord, spleen, thoracic vertebra, and liver. Treatment plans for a compact proton beam machine with single-field optimization PBS (Proteus® One, Ion Beam Applications S.A., Belgium) were generated using two different techniques. The characteristics of the treatment machine were described in detail [21–23]. The FIF technique consisted of one main field and one sub-field. The prescribed dose to the main field encompassing IGTV and ICTV was 46 Gy (RBE). The prescribed dose to the sub-field encompassing only IGTV was 14 Gy(RBE). The SIB technique consisted of only one field encompassing IGTV and ICTV. A total of 90 initial treatment plans for fifteen patients were generated. The treatment planning was conducted in the RayStation planning system version 10.0 (RaySearch Laboratories, Stockholm, Sweeden). The Monte Carlo dose calculation algorithm version 5.0 was used in the RayStation planning system version 10.0. The calculation settings were as follows: Monte Carlo optimization with 10,000 ions/spot, a dose grid of 2.0 mm, and a final dose calculation uncertainty of 0.5 %. The RBE value of 1.1 was used. In the following context, the FIF and SIB techniques using two, three, and four beams were expressed as FIF-2-beam, SIB-2-beam, FIF-3-beam, SIB-3-beam, FIF-4-beam, and SIB-4-beam, respectively. The beam incidence directions in FIF-2-beam and SIB-2-beam were two dorsal beams with gantry angles of 150° (g150)/couch rotations of 0° (c0) and g150/c180. The beam incidence directions in FIF-3-beam and SIB-3-beam were three beams with g90/c0, g150/c0, and g150/c180. The beam incidence directions in FIF-4-beam and SIB-4-beam were four beams with g0/c0, g90/c0, g180/c0, and g90/c180 following the beam arrangement of the previous studies [15,16] and the irradiation techniques used in other Japanese proton therapy facilities. Fig. 1 shows a representative example of dose distribution of a patient with the tumor in the pancreas head. The dose constraints for IGTV and ICTV were as follows[24]: (a) $D_{95\%}$ [Gy(RBE)] $\geq$ 99 % and $\leq$ 101 % of the prescribed dose; (b) $V_{100\%}$ [%] $\geq$ 90 % of the IGTV/ICTV volume; (c) $D_{2\%}$ $\leq$115 % of the prescribed dose (IGTV); and (d) $D_{2\%}$ $\leq$125 % of the prescribed dose (ICTV). The dose constraints for the stomach and duodenum were as follows: (1) $D^3_{2cm} \leq 60$ Gy(RBE); (2) stomach $V_{40Gy(RBE)} \leq 60$ cm^3; and (3) duodenum $V_{40Gy(RBE)} \leq 40$ cm^3. The constraints for other organs were equal to those of normal tissues in three-dimensional conformal radiotherapy [25]. A robust optimization with a setup robustness of 5 mm and a range uncertainty of 3.5 % was performed in the initial treatment plan. The robust optimization was applied for the IGTV and the ICTV in the initial treatment plan. The homogeneity index (HI) was defined as $D_{1\%}/D_{99\%}$. The conformity index (CI) was defined as $V_{PTV}/TV_{PV} \times V_{TV}/TV_{PV}$ (V_{PTV}, target volume; V_{TV}, treatment volume of the prescribed isodose lines; TV_{PV}, volume of V_{PTV} within the V_{TV}). An experienced medical physicist created the treatment plans, which were approved by an experienced medical doctor. One or two gold fiducial markers (Gold Anchor; GA Japan Company, Tokyo, Japan) were implanted in the pancreatic cancer lesion, and daily patient alignments were achieved by matching the fiducial markers using X-ray beams systems installed on the Proteus® One (Adapt Insight version 2.1.1.0) at the end-expiratory phase. See (Fig. 2).

The robustness evaluation for the stomach and duodenum in proximity to the IGTV and ICTV was performed because the toxicity of the stomach and duodenum were most clinically important. Dose changes resulting from range uncertainty were calculated using robustness evaluation considering range uncertainties of $\pm$ 3.5 % but no setup uncertainty. The differences in $V_{40Gy(RBE)}$ and D^3_{2cm} of the stomach and duodenum between the initial treatment plan and robustness evaluation plan were analyzed. Verification CT (vCT) scans were conducted three times, on treatment day 1, 7, and 16 (verification 1, 2, and 3: day 9, 17, and 31 after planning CT acquisition) to investigate the effect of changes in the anatomy. Rigid registration using the fiducial markers at the end-expiratory phase was performed between planning and vCT. Thereafter, the treatment plan was recalculated on the rigidly registered vCTs (interfractional dose evaluation). IGTV, ICTV, and OARs were delineated on all vCTs. $V_{100\%}$ and $D_{95\%}$ were evaluated for IGTV and ICTV on the initial and all vCTs. The parameters of D^3_{2cm} and $V_{40Gy(RBE)}$ were evaluated for the stomach and duodenum, and $D_{50\%}$ and $D_{2\%}$ were evaluated for other OARs.

2.3. Statistical data analyses

The Wilcoxon signed-rank test was used to compare each pair of dose–volume parameters for the initial treatment plans and interfractional dose evaluations, and the Benjamini-Hochberg correction was used for multiple comparisons. The non-parametric Friedman test was used to compare dose-volume parameters among different techniques. A

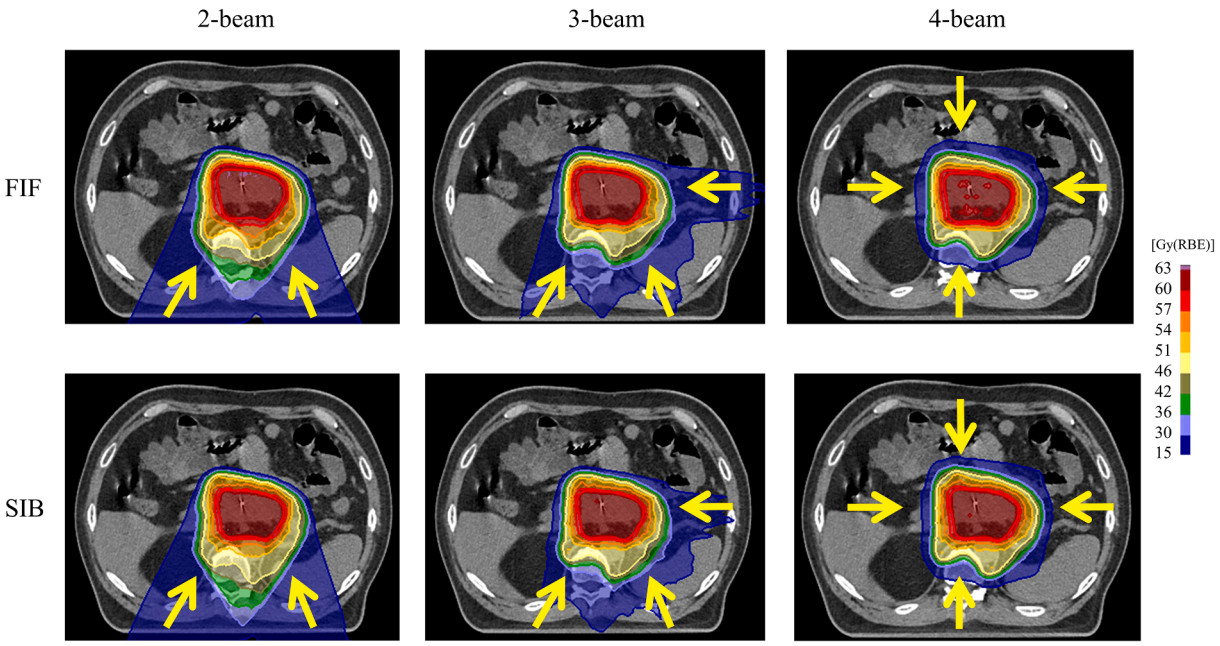

Fig. 1. A representative example of dose distribution. Yellow arrows represent beam angles.

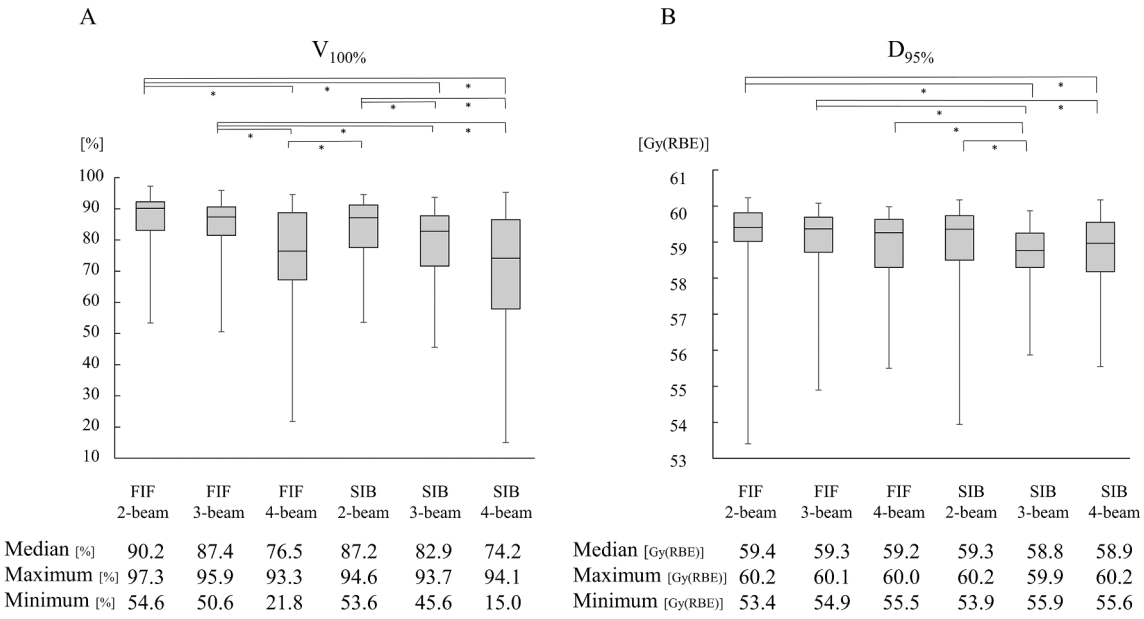

	FIF 2-beam	FIF 3-beam	FIF 4-beam	SIB 2-beam	SIB 3-beam	SIB 4-beam
Median [%]	90.2	87.4	76.5	87.2	82.9	74.2
Maximum [%]	97.3	95.9	93.3	94.6	93.7	94.1
Minimum [%]	54.6	50.6	21.8	53.6	45.6	15.0

	FIF 2-beam	FIF 3-beam	FIF 4-beam	SIB 2-beam	SIB 3-beam	SIB 4-beam
Median [Gy(RBE)]	59.4	59.3	59.2	59.3	58.8	58.9
Maximum [Gy(RBE)]	60.2	60.1	60.0	60.2	59.9	60.2
Minimum [Gy(RBE)]	53.4	54.9	55.5	53.9	55.9	55.6

Fig. 2. Box plots for dose-volume parameters for recalculated IGTV over all interfractional dose evaluations. The boxes contain data of all three interfractional dose evaluations (n = 45). (A) $V_{100\%}$; the dose constraint is $V_{100\%} \geq 90$ %. (B) $D_{95\%}$; the dose constraint is 59.4 Gy(RBE) $\leq D_{95\%} \leq$ 60.6 Gy(RBE); the median, maximum, and minimum below the Figure indicates to the median value, maximum value, and minimum value of box plots for $V_{100\%}$ and $D_{95\%}$, respectively. The symbol (*) indicates significant differences.

p value < 0.05 was considered to indicate a significant difference. All statistical analyses were conducted using open-source software, R Version 4.1.3 (The R Foundation for Statistical Computing, Vienna, Austria).

3. Results

3.1. Dose-volume parameters of the target

The dose-volume parameters for the IGTV and ICTV for the initial treatment plans and the recalculations on the vCTs are summarized in Table 1. There was no significant difference for the HI among different techniques. The CI of ICTV for the FIF-4-beam technique was better by 10.5 % and 8.0 % compared to the FIF-2-beam and FIF-3-beam techniques ($p = 0.004$ and $p = 0.021$). The CI of ICTV for the SIB-4-beam technique was better by 14.9 % and 7.0 % compared to the SIB-2-beam and SIB-3-beam techniques ($p = 0.002$ and $p = 0.004$). The $V_{100\%}$ and $D_{95\%}$ parameters of IGTV significantly decreased in all interfractional dose evaluations compared to those in the initial treatment plan ($p < 0.001$) as depicted in Figure S1 and S2. The FIF-2-beam, FIF-3-beam, and SIB-2-beam techniques maintained the highest IGTV $V_{100\%}$ and $D_{95\%}$. The IGTV $V_{100\%}$ and the $D_{95\%}$ parameters significantly decreased for the recalculation on all three vCTs. The ICTV $V_{100\%}$ and the $D_{95\%}$ parameters significantly decreased for the recalculation on vCT

Table 1
Target dose-volume parameters in the initial treatment plan, verification 1, verification 2, and verification 3. All parameters are presented as median (range).

IGTV	HI, CI	Parameter	Initial plan	Verification 1	Verification 2	Verification 3
FIF-2-beam	1.05 (1.03–1.07), 1.19 (1.10–1.39)	$V_{100\%}$ [%]	96.1 (92.6–97.6)	91.8 (75.6–97.3)	90.0 (77.5–93.7)	85.6 (54.6–95.2)
		$D_{95\%}$ [Gy(RBE)]	60.0 (59.8–60.2)	59.6 (58.2–60.2)	59.4 (57.2–60.0)	59.3 (53.4–60.0)
FIF-3-beam	1.04 (1.03–1.07),	$V_{100\%}$ [%]	95.5 (91.2–99.5)	87.7 (68.9–95.3)	86.7 (74.4–95.8)	84.9 (50.6–95.9)
	1.18 (1.10–1.32)	$D_{95\%}$ [Gy(RBE)]	60.0 (59.7–60.5)	59.4 (57.4–60.0)	59.3 (57.6–60.1)	59.1 (54.9–60.1)
FIF-4-beam	1.03 (1.02–1.22),	$V_{100\%}$ [%]	95.2 (92.8–98.3)	78.9 (45.8–93.3)	81.5 (55.2–92.2)	73.2 (21.8–92.2)
	1.18 (1.10–1.36)	$D_{95\%}$ [Gy(RBE)]	60.0 (59.9–60.4)	59.3 (57.6–59.9)	59.4 (57.3–60.0)	59.2 (55.5–59.8)
SIB-2-beam	1.05 (1.04–1.07),	$V_{100\%}$ [%]	95.1 (93.9–98.0)	88.9 (70.3–94.6)	86.7 (75.3–92.3)	82.1 (53.6–94.1)
	1.17 (1.08–1.26)	$D_{95\%}$ [Gy(RBE)]	60.0 (59.9–60.3)	59.4 (57.5–60.0)	59.2 (57.2–60.0)	58.8 (53.9–60.2)
SIB-3-beam	1.05 (1.04–1.07),	$V_{100\%}$ [%]	95.0 (95.0–98.0)	75.0 (54.5–93.7)	84.5 (64.1–91.7)	79.8 (45.6–91.9)
	1.13 (1.08–1.19)	$D_{95\%}$ [Gy(RBE)]	60.0 (60.0–60.3)	58.7 (57.7–59.9)	58.8 (57.0–59.7)	58.7 (55.9–59.8)
SIB-4-beam	1.04 (1.03–1.06),	$V_{100\%}$ [%]	95.6 (95.0–98.1)	72.5 (48.4–90.1)	79.4 (15.0–94.1)	66.4 (18.0–93.3)
	1.15 (1.07–1.22)	$D_{95\%}$ [Gy(RBE)]	60.0 (60.0–60.4)	58.7 (57.0–60.0)	59.3 (56.3–60.0)	58.6 (55.6–60.2)
ICTV	HI, CI	Parameter	Initial plan	Verification 1	Verification 2	Verification 3
FIF-2-beam	1.35 (1.33–1.37),	$V_{100\%}$ [%]	96.5 (94.0–100)	95.2 (79.0–98.7)	93.3 (77.1–99.4)	94.2 (78.0–100)
	1.80 (1.62–2.36)	$D_{95\%}$ [Gy(RBE)]	46.3 (45.8–46.4)	46.1 (45.5–47.7)	45.7 (42.8–47.3)	45.8 (41.7–46.6)
FIF-3-beam	1.35 (1.33–1.43),	$V_{100\%}$ [%]	96.5 (94.2–100)	95.9 (71.1–98.3)	94.4 (71.6–98.6)	93.4 (74.1–100)
	1.75 (1.51–2.24)	$D_{95\%}$ [Gy(RBE)]	46.2 (45.8–46.4)	46.1 (45.1–46.7)	45.7 (41.9–46.4)	45.7 (41.9–46.5)
FIF-4-beam	1.34 (1.33–1.41),	$V_{100\%}$ [%]	96.3 (91.6–100)	94.5 (64.0–99.5)	94.3 (85.1–98.1)	93.9 (82.4–99.9)
	1.61 (1.42–2.15)	$D_{95\%}$ [Gy(RBE)]	46.4 (45.8–46.4)	46.0 (45.2–46.8)	45.7 (43.0–46.4)	45.6 (42.3–46.6)
SIB-2-beam	1.34 (1.32–1.38),	$V_{100\%}$ [%]	95.9 (93.2–100)	95.4 (77.1–99.4)	95.3 (74.0–99.9)	93.5 (80.2–100)
	1.88 (1.64–2.38)	$D_{95\%}$ [Gy(RBE)]	46.1 (45.9–46.4)	46.1 (45.8–46.4)	46.0 (45.2–46.4)	46.0 (44.3–46.4)
SIB-3-beam	1.33 (1.32–1.37),	$V_{100\%}$ [%]	96.0 (94.9–99.9)	94.9 (74.4–98.9)	94.3 (83.5–98.2)	92.4 (80.2–99.9)
	1.72 (1.50–2.28)	$D_{95\%}$ [Gy(RBE)]	46.1 (45.6–46.4)	45.8 (45.0–46.2)	45.8 (43.7–46.2)	45.6 (43.2–46.5)
SIB-4-beam	1.33 (1.32–1.36),	$V_{100\%}$ [%]	96.3 (94.1–99.9)	95.0 (59.9–98.8)	94.4 (73.2–97.7)	93.7 (80.0–99.6)
	1.60 (1.53–2.21)	$D_{95\%}$ [Gy(RBE)]	46.2 (45.9–46.4)	46.1 (44.9–46.4)	45.9 (42.9–46.4)	45.8 (42.8–46.5)

Abbreviations: IGTV, internal gross tumor volume; ICTV, internal clinical target volume; FIF, field-in-field; SIB, simultaneous integrated boost; RBE, relative biological effectiveness; HI, homogeneity index; CI, conformity index.

2 and 3. The significance values for the comparison of the initial doses and the interfractional evaluation doses for all treatment techniques are summarized in Table S2.

3.2. Dose-volume parameters of OARs, and robustness evaluation for stomach and duodenum

The OARs dose-volume parameters in the initial treatment plans are summarized in Table 2. The $D_{50\%}$ and $D_{2\%}$ of the small and large bowels were the lowest when only using two beams, for both treatment concepts. The $D_{50\%}$ and $D_{2\%}$ of the kidneys, spinal cord, and thoracic

Table 2
Dose-volume parameters of organs at risk in the initial treatment plans. All parameters are presented as median (range).

	FIF-2-beam	FIF-3-beam	FIF-4-beam	SIB-2-beam	SIB-3-beam	SIB-4-beam
Stomach						
$V_{40Gy(RBE)}$ [cm^3]	3.8 (0–46.5)	5.0 (0–47.7)	7.0 (0–50.7)	5.2 (0–54.4)	4.7 (0–56.1)	5.7 (0–54.6)
D^3_{2cm} [Gy(RBE)]	43.6 (4.6–57.6)	47.6 (5.9–57.2)	46.7 (16.0–58.2)	46.2 (4.9–58.0)	45.9 (6.1–57.0)	48.3 (15.4–58.6)
Duodenum						
$V_{40Gy(RBE)}$ [cm^3]	6.2 (0–29.5)	7.0 (0–27.8)	6.9 (0–29.3)	6.1 (0–30.7)	6.5 (0–28.0)	6.5 (0–32.5)
D^3_{2cm} [Gy(RBE)]	49.2 (28.0–56.2)	49.4 (18.7–57.1)	48.9 (29.3–54.8)	49.9 (25.7–55.5)	51.1 (22.2–56.6)	48.8 (28.7–54.2)
Small bowel						
$D_{50\%}$ [Gy(RBE)]	4.1 (1.8–29.5)	11.2 (1.5–35.5)	12.1 (7.6–35.9)	4.2 (1.8–32.2)	11.0 (1.7–37.7)	11.8 (7.1–36.6)
$D_{2\%}$ [Gy(RBE)]	42.1 (24.0–49.2)	42.5 (21.6–51.9)	42.2 (20.4–51.1)	40.8 (24.5–48.4)	41.8 (19.8–52.5)	42.6 (22.7–52.1)
Large bowel						
$D_{50\%}$ [Gy(RBE)]	0.1 (0–12.5)	4.2 (0–15.0)	6.2 (3.1–21.0)	0.1 (0–13.9)	4.3 (0–16.2)	6.1 (3.1–20.7)
$D_{2\%}$ [Gy(RBE)]	1.6 (0.1–50.2)	15.7 (0.1–50.1)	12.1 (11.0–49.7)	1.9 (0.1–53.4)	14.8 (0.1–51.7)	12.0 (10.6–50.9)
Kidney (right)						
$D_{50\%}$ [Gy(RBE)]	11.4 (3.2–19.6)	9.6 (2.2–14.7)	1.9 (0.4–16.7)	12.0 (1.5–21.2)	8.3 (3.5–19.9)	1.8 (0.4–17.3)
$D_{2\%}$ [Gy(RBE)]	26.7 (18.6–40.2)	18.1 (12.9–38.7)	12.7 (4.9–30.1)	24.8 (17.7–41.1)	18.3 (12.7–32.8)	11.3 (5.2–27.5)
Kidney (left)						
$D_{50\%}$ [Gy(RBE)]	13.0 (1.6–21.3)	9.1 (3.6–20.5)	3.0 (0.4–16.7)	12.8 (1.5–21.2)	9.7 (3.5–19.9)	3.4 (0.4–17.3)
$D_{2\%}$ [Gy(RBE)]	33.9 (20.4–52.8)	29.7 (13.2–52.7)	25.3 (5.9–51.9)	33.6 (19.5–52.5)	28.5 (12.9–50.9)	24.9 (7.1–53.3)
Spinal cord						
$D_{50\%}$ [Gy(RBE)]	21.5 (13.5–28.1)	14.5 (8.4–19.0)	7.0 (4.7–9.7)	21.8 (14.1–28.1)	14.1 (9.4–19.0)	6.9 (5.0–9.3)
$D_{2\%}$ [Gy(RBE)]	36.8 (24.0–38.8)	24.8 (15.3–26.7)	10.7 (9.8–15.4)	36.9 (26.6–39.7)	24.0 (17.6–26.1)	9.9 (9.3–16.7)
Spleen						
$D_{50\%}$ [Gy(RBE)]	4.8 (0–17.9)	3.4 (0–16.9)	0.5 (0–12.5)	5.1 (0–17.8)	3.4 (0–16.8)	0.5 (0–12.3)
$D_{2\%}$ [Gy(RBE)]	17.2 (0–42.3)	12.2 (0–42.8)	5.9 (0–38.6)	16.8 (0–43.8)	11.9 (0–41.4)	6.8 (0–39.1)
Thoracic vertebra						
$D_{50\%}$ [Gy(RBE)]	28.4 (21.6–38.2)	22.7 (14.5–30.8)	15.4 (9.5–23.3)	29.7 (20.7–39.0)	22.4 (14.7–30.8)	15.7 (9.3–24.2)
$D_{2\%}$ [Gy(RBE)]	48.2 (45.1–51.7)	46.1 (37.7–49.5)	44.1 (32.2–47.0)	48.4 (41.6–52.3)	45.8 (37.7–49.3)	45.2 (33.0–47.7)
Liver						
$D_{50\%}$ [Gy(RBE)]	1.8 (0.1–4.2)	1.7 (0.1–4.0)	3.4 (0.1 –6.6)	1.8 (0.1–4.3)	1.8 (0.1–3.8)	3.2 (0.1–6.6)
$D_{2\%}$ [Gy(RBE)]	24.3 (0.1–42.4)	25.3 (8.1–41.4)	29.6 (9.0–41.9)	25.7 (1.0–42.2)	23.2 (10.0–42.5)	27.4 (8.9–42.5)

Abbreviations: FIF, field-in-field; SIB, simultaneous integrated boost; RBE, relative biological effectiveness.

vertebra could be reduced the most when using four beams. The significance values for the comparison of the initial doses of OARs among different techniques are summarized in Table S3. No significant difference was observed between both treatment concepts with the same number of beams.

The data of the robustness evaluation for the stomach and duodenum dose-volume parameters in the initial treatment plan are summarized in Table S4. For the stomach, the two-beam technique with a range uncertainty of −3.5 % showed the highest median ΔD^3_{2cm} ($p < 0.05$, compared to three-beam and four-beam techniques, for both treatment concepts). For the duodenum, the four-beam technique with a range uncertainty of −3.5 % showed the highest median ΔD^3_{2cm} ($p < 0.05$, compared to two-beam and three-beam techniques, for both treatment concepts). Fig. 3 shows a representative example of robustness evaluation for FIF-2-beam and SIB-2-beam techniques.

4. Discussion

This was the first study to investigate treatment strategies employing various beam directions of FIF and SIB techniques using PBS for pancreatic cancer and to evaluate the changes in target coverage based on recalculations on three vCTs. This study revealed that IGTV coverage of PBS proton therapy considerably decreased due to the effect of changes in the anatomy. These include interfractional positional changes of the pancreas [26,27] and changes in intestinal gas volume [28–30]. A two-beam technique could achieve a high target coverage while reducing the dose to small and the large bowels better than using three or four beams for both treatment concepts. The reason was that the beams did not pass through the bowels. On the other hand, the $D_{50\%}$ and $D_{2\%}$ for organs located on the dorsal side (kidneys, spinal cord, and thoracic vertebra) in the two-beam techniques were the highest compared to the three-beam and four-beam techniques, for both treatment concepts. The doses to the stomach in the FIF-2-beam and SIB-2-beam techniques, as well as the doses to the duodenum in the FIF-4-beam and SIB-4-beam techniques, showed the greatest variability. More beams produced more robust plans in general. However, treatment plans using four-beam technique resulted in the largest dose variations for the duodenum. This variability could potentially lead to unexpected complications such as gastrointestinal ulcers, hemorrhage, and perforation in the worst case. In proton therapy for pancreatic cancer, the gastrointestinal toxicity risk remains high [31,32], prompting various studies aimed to reduce the toxicity risk [33,34]. Robustness evaluations for the stomach and duodenum during the treatment plan creation is one approach to mitigate dose uncertainties. Beam arrangements considering the minimization of dose variability in the stomach and duodenum are necessary to reduce the toxicity risk. Adaptive planning is an increasing concern in particle therapy [35]. However, the optimal method has not fully been established [36,37]. Through recalculation on vCTs, it may be necessary to conduct re-planning at the beginning of treatment in some cases.

Three-beam techniques were recommended in a previous study [16]. The results of our study are consistent with those findings. The FIF-3-beam and SIB-3-beam techniques may be the most appropriate, considering IGTV coverage and the sparing of OARs comprehensively. The IGTV coverage of the FIF-3-beam technique was slightly higher than that of the SIB-3-beam technique. However, intermittent irradiation was required with the FIF technique due to the need for time intervals between the main field and sub-field irradiation. The time intervals between the main field and sub-field irradiation may require about five minutes due to gantry rotation, fiducial markers re-matching, and stabilization of respiratory cycles. Intermittent irradiation may result in the anti-tumor effect reduction due to the recovery from sublethal damage [38–40]. The SIB-3-beam technique has been used in clinical treatment for pancreatic cancer at our facility. Although FIF techniques are not commonly used, the results of this study suggest that FIF techniques may be worth considering in some situations to prevent the decrease of target coverage. Further studies are needed to establish which patients benefit the most by the use of FIF techniques and the quality of FIF techniques should be assessed in detail. Dose escalation has been attempted in particle therapy for pancreatic cancer to improve local control [41,42]. The study results could provide useful information to determine the beam arrangement of PBS proton therapy for pancreatic cancer.

This study had several limitations. First, the number of evaluated patients was relatively small, and thus a larger sample size is needed for a more detailed analysis. Second, the intrafractional motions of the organs and the intestinal gas that affect target and OAR doses were not evaluated. The target coverage might be further reduced due to intrafractional motions of the organs and the intestinal gas during irradiation. There are several recent studies dealing with this topic [43,44]. Third, the robustness evaluation of the stomach and duodenum was

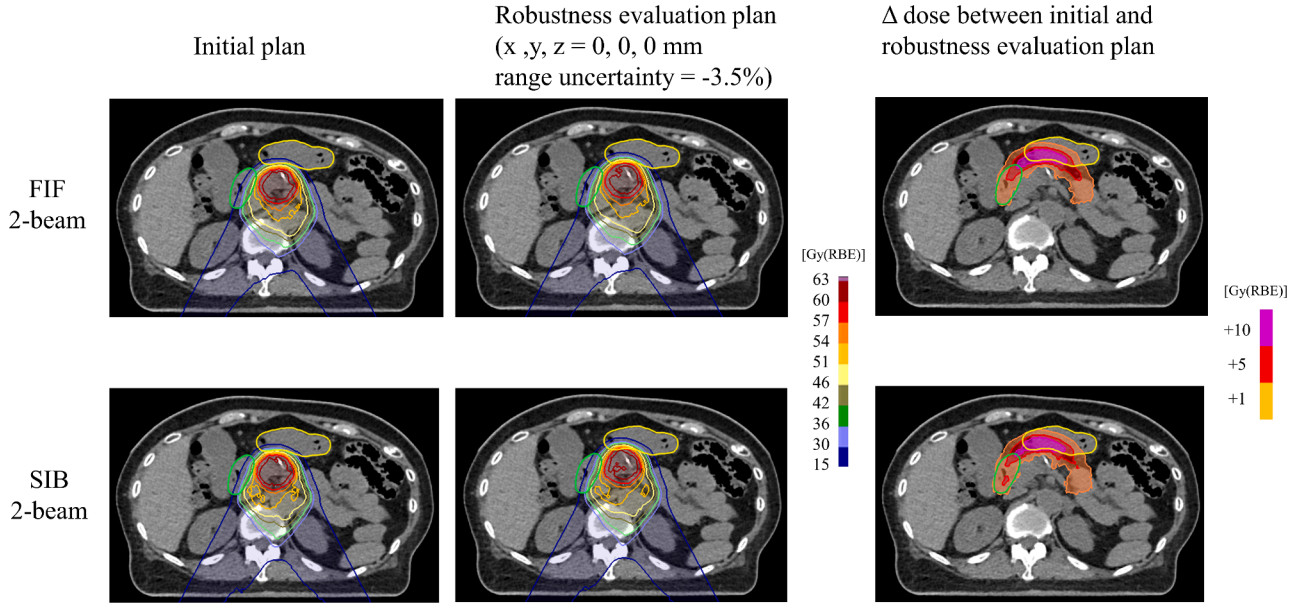

Fig. 3. A representative example of robustness evaluation in FIF-2-beam and SIB-2-beam techniques. Yellow contours represent the stomach. Green contours represent the duodenum.

conducted, considering only the range uncertainty, without considering motions of the targets and organs.

In conclusion, IGTV coverage recalculated on three CTs during treatment decreased for both treatment concepts. The FIF with three beams technique maintained the highest IGTV coverage and achieved the sparing of normal organs the most.

5. Declaration of generative AI in scientific writing

The authors declare no use of generative AI and AI-assisted technologies in the writing.

6. Date availability statement

The data that support the findings of this study are available on request from the corresponding author. The data are not publicly available due to restrictions such as their containing information that could compromise the privacy of research participants.

7. Ethics statement

This study was performed after approval by the institutional review board of Narita Memorial Hospital (approval number: R041041). Written informed consent was obtained from all patients and has been conducted in compliance with the guidelines of the Helsinki Declaration.

CRediT authorship contribution statement

Taiki Takaoka: Conceptualization, Data curation, Investigation, Writing – original draft. **Takeshi Yanagi:** Data curation, Formal analysis. **Shinsei Takahashi:** Data curation, Investigation. **Yuta Shibamoto:** Writing – review & editing. **Yuto Imai:** Data curation. **Dai Okazaki:** Formal analysis. **Masanari Niwa:** Formal analysis. **Akira Torii:** Formal analysis. **Nozomi Kita:** Formal analysis. **Seiya Takano:** Data curation. **Natsuo Tomita:** Writing – review & editing. **Akio Hiwatashi:** Writing – review & editing.

Declaration of competing interest

The authors declare that they have no known competing financial interests or personal relationships that could have appeared to influence the work reported in this paper.

Acknowledgments

This work was supported by JSPS KAKENHI Grant Number 24K18769. We would like to thank all staffs at our hospital.

Appendix A. Supplementary data

Supplementary data to this article can be found online at https://doi.org/10.1016/j.phro.2024.100583.

References

[1] Yanagi T, Takama N, Kato E, Baba F, Kitase M, Shimohira M, et al. Clinical outcomes of intraoperative radiotherapy, postoperative radiotherapy, and definitive radiotherapy for non-metastatic pancreatic cancer. Kurume Med J 2023;67:163–70. https://doi.org/10.2739/kurumemedj.MS674002.

[2] Karasawa K, Sunamura M, Okamoto A, Nemoto K, Matsuno S, Nishimura Y, et al. Efficacy of novel hypoxic cell sensitiser doranidazole in the treatment of locally advanced pancreatic cancer: long-term results of a placebo-controlled randomised study. Radiother Oncol 2008;87:326–30. https://doi.org/10.1016/j.radonc.2008.02.007.

[3] Hammel P, Huguet F, van Laethem JL, Goldstein D, Glimelius B, Artru P, et al. Effect of chemoradiotherapy vs chemotherapy on survival in patients with locally advanced pancreatic cancer controlled after 4 months of gemcitabine with or without erlotinib: the LAP07 randomized clinical trial. JAMA 2016;315:1844–53. https://doi.org/10.1001/jama.2016.4324.

[4] Ogura Y, Terashima K, Nanno Y, Park S, Suga M, Takahashi D, et al. Factors associated with long-term survival in gemcitabine-concurrent proton radiotherapy for non-metastatic locally advanced pancreatic cancer: a single-center retrospective study. Radiat Oncol 2022;17:32. https://doi.org/10.1186/s13014-022-02001-w.

[5] Hagiwara Y, Bhattacharyya T, Matsufuji N, Isozaki Y, Takiyama H, Nemoto K, et al. Influence of dose-averaged linear energy transfer on tumour control after carbon-ion radiation therapy for pancreatic cancer. Clin Transl Radiat Oncol 2019;21:19–24. https://doi.org/10.1016/j.ctro.2019.11.002.

[6] Shinoto M, Yamada S, Terashima K, Yasuda S, Shioyama Y, Honda H, et al. Carbon ion radiation therapy with concurrent gemcitabine for patients with locally advanced pancreatic cancer. Int J Radiat Oncol Biol Phys 2016;95:498–504. https://doi.org/10.1016/j.ijrobp.2015.12.362.

[7] Lühr A, von Neubeck C, Krause M, Troost EGC. Relative biological effectiveness in proton beam therapy – Current knowledge and future challenges. Clin Transl Radiat Oncol 2018;9:35–41. https://doi.org/10.1016/j.ctro.2018.01.006.

[8] Ding X, Dionisi F, Tang S, Ingram M, Hung CY, Prionas E, et al. A comprehensive dosimetric study of pancreatic cancer treatment using three-dimensional conformal radiation therapy (3DCRT), intensity-modulated radiation therapy (IMRT), volumetric-modulated radiation therapy (VMAT), and passive-scattering and modulated-scanning proton therapy (PT). Med Dosim 2014;39:139–45. https://doi.10.1016/j.meddos.2013.11.005.

[9] Kumagai M, Hara R, Mori S, Yanagi T, Asakura H, Kishimoto R, et al. Impact of intrafractional bowel gas movement on carbon ion beam dose distribution in pancreatic radiotherapy. Int J Radiat Oncol Biol Phys 2009;73:1276–81. https://doi.org/10.1016/j.ijrobp.2008.10.055.

[10] Houweling AC, Fukata K, Kubota Y, Shimada H, Rasch CR, Ohno T, et al. The impact of interfractional anatomical changes on the accumulated dose in carbon ion therapy of pancreatic cancer patients. Radiother Oncol 2016;119:319–25. https://doi.org/10.1016/j.radonc.2016.03.004.

[11] Knäusl B, Lebbink F, Fossati P, Engwall E, Georg D, Stock M. Patient breathing motion and delivery specifics influencing the robustness of a proton pancreas irradiation. Cancers (Basel) 2023;15:2550. https://doi.org/10.3390/cancers15092550.

[12] Ribeiro CO, Meijers A, Korevaar EW, Muijs CT, Both S, Langendijk JA, et al. Comprehensive 4D robustness evaluation for pencil beam scanned proton plans. Radiother Oncol 2019;136:185–9. https://doi.org/10.1016/j.radonc.2019.03.037.

[13] Batista V, Richter D, Combs SE, Jakel O. Planning strategies for inter-fractional robustness in pancreatic patients treated with scanned carbon therapy. Radiat Oncol 2017;12:94. https://doi.org/10.1186/s13014-017-0832-x.

[14] Dreher C, Habermehl D, Ecker S, Brons S, El-Shafie R, Jäkel O, et al. Optimization of carbon ion and proton treatment plans using the raster-scanning technique for patients with unresectable pancreatic cancer. Radiat Oncol 2015;10:237. https://doi.org/10.1186/s13014-015-0538-x.

[15] Koom WS, Mori S, Furuich W, Yamada S. Beam direction arrangement using a superconducting rotating gantry in carbon ion treatment for pancreatic cancer. Br J Radiol 2019;92:20190101. https://doi.org/10.1259/bjr.20190101.

[16] Stefanowicz S, Stützer K, Zschaeck S, Jakobi A, Troost EGC. Comparison of different treatment planning approaches for intensity-modulated proton therapy with simultaneous integrated boost for pancreatic cancer. Radiat Oncol 2018;13:228. https://doi.org/10.1186/s13014-018-1165-0.

[17] den Otter LA, Anakotta RM, Weessies M, Roos CTG, Sijtsema NM, Muijs CT, et al. Investigation of inter-fraction target motion variations in the context of pencil beam scanned proton therapy in non-small cell lung cancer patients. Med Phys 2020;47:3835–44. https://doi.org/10.1002/mp.14345.

[18] Spautz S, Haase L, Tschiche M, Makocki S, Richter C, Troost EGC, et al. Comparison of 3D and 4D robustly optimized proton treatment plans for non-small cell lung cancer patients with tumour motion amplitudes larger than 5 mm. Phys Imaging Radiat Oncol 2023;27:100465. https://doi.org/10.1016/j.phro.2023.100465.

[19] Hijal T, Fournier-Bidoz N, Castro-Pena P, Kirova YM, Zefkili S, Bollet MA, et al. Simultaneous integrated boost in breast conserving treatment of breast cancer: A dosimetric comparison of helical tomotherapy and three-dimensional conformal radiotherapy. Radiother Oncol 2010;94:300–6. https://doi.10.1016/j.radonc.2009.12.043.

[20] Joseph B, Farooq N, Kumar S, Vijay CR, Puthur KJ, Ramesh C, et al. Breast-conserving radiotherapy with simultaneous integrated boost; field-in-field three-dimensional conformal radiotherapy versus inverse intensity-modulated radiotherapy – a dosimetric comparison: do we need intensity-modulated radiotherapy? South Asian. J Cancer 2018;7:163–6. https://doi.org/10.4103/sajc.sajc_82_18.

[21] Pidikiti R, Patel BC, Maynard MR, Dugas JP, Syh J, Sahoo N, et al. Commissioning of the world's first compact pencil-beam scanning proton therapy system. J Appl Clin Med Phys 2018;19:94–105. https://doi.org/10.1002/acm2.12225.

[22] Mizuno T, Tomita N, Takaoka T, Tomida M, Fukuma H, Tsuchiya T, et al. Dosimetric comparison of helical tomotherapy, volumetric-modulated arc therapy, and intensity-modulated proton therapy for angiosarcoma of the scalp. Technol Cancer Res Treat 2021;20:1533033820985866. https://doi.org/10.1177/1533033820985866.

[23] Takaoka T, Yanagi T, Tanaka A, Kiriyama Y, Tanaka Y, Kondo T, et al. Acute genitourinary toxicity of pencil beam scanning proton therapy for localized prostate cancer: utility of the transition zone index and average urinary flow rate in predicting acute urinary retention. Jpn J Clin Oncol 2023;53:419–28. https://doi.org/10.1093/jjco/hyad005.

[24] Doppenberg D, Lagerwaard FJ, van Dieren S, Meijerink MR, van der Vliet JJ, Besselink MG, et al. Optimizing patient selection for stereotactic ablative

radiotherapy in patients with locally advanced pancreatic cancer after initial chemotherapy - a single center prospective cohort. Front Oncol 2023;13:1149961. https://doi.org/10.3389/fonc.2023.1149961.
[25] Emami B, Lyman J, Brown A, Coia L, Goitein M, Munzenrider JE, et al. Tolerance of normal tissue to therapeutic irradiation. Int J Radiat Oncol Biol Phys 1991;21:109–22. https://doi.org/10.1016/0360-3016(91)90171-y.
[26] Hendifar AE, Petzel MQB, Zimmers TA, Denlinger CS, Matrisian LM, Picozzi VJ, et al. Pancreas cancer-associated weight loss. Oncologist 2019;24:691–701. https://doi.org/10.1634/theoncologist.2018-0266.
[27] Takeda T, Sasaki T, Mie T, Furukawa T, Yamada Y, Kasuga A, et al. The impact of body composition on short-term outcomes of neoadjuvant chemotherapy with gemcitabine plus S-1 in patients with resectable pancreatic cancer. Jpn J Clin Oncol 2021;51:604–11. https://doi.org/10.1093/jjco/hyaa247.
[28] van der Horst A, Houweling AC, van Tienhoven G, Visser J, Bel A. Dosimetric effects of anatomical changes during fractionated photon radiation therapy in pancreatic cancer patients. J Appl Clin Med Phys 2017;18:142–51. https://doi.org/10.1002/acm2.12199.
[29] Narita Y, Kato T, Takemasa K, Sato H, Ikeda T, Harada T, et al. Dosimetric impact of simulated changes in large bowel content during proton therapy with simultaneous integrated boost for locally advanced pancreatic cancer. J Appl Clin Med Phys 2021;22:90–8. https://doi.org/10.1002/acm2.13429.
[30] Uchinami Y, Kanehira T, Fujita Y, Miyamoto N, Yokokawa K, Koizumi F, et al. Evaluation of short-term gastrointestinal motion and its impact on dosimetric parameters in stereotactic body radiation therapy for pancreatic cancer. Clin Transl Radiat Oncol 2023;39:100576. https://doi.org/10.1016/j.ctro.2023.100576.
[31] Takatori K, Terashima K, Yoshida R, Horai A, Satake S, Ose T, et al. Upper gastrointestinal complications associated with gemcitabine-concurrent proton radiotherapy for inoperable pancreatic cancer. J Gastroenterol 2014;49:1074–80. https://doi.org/10.1007/s00535-013-0857-3.
[32] Kobeissi JM, Simone 2nd CB, Lin H, Hilal L, Hajj C. Proton therapy in the management of pancreatic cancer. Cancers (Basel) 2022;14:2789. https://doi.org/10.3390/cancers14112789.
[33] Raturi VP, Hojo H, Hotta K, Baba H, Takahashi R, Rachi T, et al. Radiobiological model-based approach to determine the potential of dose-escalated robust intensity-modulated proton radiotherapy in reducing gastrointestinal toxicity in the treatment of locally advanced unresectable pancreatic cancer of the head. Radiat Oncol 2020;15:157. https://doi.org/10.1186/s13014-020-01592-6.
[34] Raturi VP, Tochinai T, Hojo H, Rachi T, Hotta K, Nakamura N, et al. Dose–volume and radiobiological model-based comparative evaluation of the gastrointestinal toxicity risk of photon and proton irradiation plans in localized pancreatic cancer without distant metastasis. Front Oncol 2020;10:517061. https://doi.org/10.3389/fonc.2020.517061.
[35] Trnkova P, Zhang Y, Toshito T, Heijmen B, Richter C, Aznar MC, et al. A survey of practice patterns for adaptive particle therapy for interfractional changes. Phys Imaging Radiat Oncol 2023;26:100442. https://doi.org/10.1016/j.phro.2023.100442.
[36] Kawashima M, Tashiro M, Varnava M, Shiba S, Matsui T, Okazaki S, et al. An adaptive planning strategy in carbon ion therapy of pancreatic cancer involving beam angle selection. Phys Imaging Radiat Oncol 2022;21:35–41. https://doi.org/10.1016/j.phro.2022.01.005.
[37] Taasti VT, Hattu D, Peeters S, van der Salm A, van Loon J, de Ruysscher D, et al. Clinical evaluation of synthetic computed tomography methods in adaptive proton therapy of lung cancer patients. Phys Imaging Radiat Oncol 2023;27:100459. https://doi.org/10.1016/j.phro.2023.100459.
[38] Shibamoto Y, Ito M, Sugie C, Ogino H, Hara M. Recovery from sublethal damage during intermittent exposures in cultured tumor cells: implications for dose modification in radiosurgery and IMRT. Int J Radiat Oncol Biol Phys 2004;59:1484–90. https://doi.org/10.1016/j.ijrobp.2004.04.039.
[39] Tomita N, Shibamoto Y, Ito M, Ogino H, Sugie C, Ayakawa S, et al. Biological effect of intermittent radiation exposure in vivo: recovery from sublethal damage versus reoxygenation. Radiother Oncol 2008;86:369–74. https://doi.org/10.1016/j.radonc.2007.08.007.
[40] Hashimoto S, Sugie C, Iwata H, Ogino H, Omachi C, Yasui K, et al. Recovery from sublethal damage and potentially lethal damage : Proton beam irradiation vs. X-ray irradiation Strahlenther Onkol 2018;194:343–51. https://doi.org/10.1007/s00066-017-1223-9.
[41] Stefanowicz S, Wlodarczyk W, Frosch S, Zschaeck S, Troost EGC. Dose-escalated simultaneously integrated boost photon or proton therapy in pancreatic cancer in an in-silico study: Gastrointestinal organs remain critical. Clin Transl Radiat Oncol 2020;27:24–31. https://doi.org/10.1016/j.ctro.2020.12.001.
[42] Kawashiro S, Mori S, Yamada S, Miki K, Nemoto K, Tsuji H, et al. Dose escalation study with respiratory-gated carbon-ion scanning radiotherapy using a simultaneous integrated boost for pancreatic cancer: simulation with four-dimensional computed tomography. Br J Radiol 2017;90:20160790. https://doi.org/10.1259/bjr.20160790.
[43] Zhang Y, Trnkova P, Toshito T, Heijmen B, Richter C, Aznar M, et al. A survey of practice patterns for real-time intrafractional motion-management in particle therapy. Phys Imaging Radiat Oncol 2023;26:100439. https://doi.org/10.1016/j.phro.2023.100439.
[44] Lebbink F, Stocchiero S, Fossati P, Engwall E, Georg D, Stock M, et al. Parameter based 4D dose calculations for proton therapy. Phys Imaging Radiat Oncol 2023;27:100473. https://doi.org/10.1016/j.phro.2023.100473.